



Anal. Bioanal. Chem. Res., Vol. 7, No. 4, 445-460, September 2020.

One New Azo-azomethine Derivative for Detection of Ca^{2+} and Cd^{2+} Metal Ions: Synthesis, Characterization and DFT Studies

Zohreh Shaghghi* and Mina Kheyrollahpoor

*Coordination Chemistry Research Laboratory, Department of Chemistry, Faculty of Basic Science, Azarbaijan Shahid Madani University,
P. O. Box: 83714-161, Tabriz, Iran*

(Received 25 October 2019 Accepted 2 May 2020)

One new azo Schiff-base derivative, 4-bromo-1,2-bis[2-hydroxy-5-(phenylazo)benzylideneamino]benzene (H_2L), was synthesized and characterized by common spectroscopic techniques and elemental analysis. The ability of the new chemosensor for detection of some main and transition metal ions was studied by UV-Vis spectroscopy in the mixture of DMSO: water (9:1). Upon addition of Ca^{2+} and Cd^{2+} ions, dramatic changes were observed in the UV-Vis spectrum of ligand (one new absorption band appeared in the range of 430-450 nm, while the absorption band at 351 nm disappeared). The stoichiometry of the complexes was determined using the Job method. The binding constants of Ca^{2+} and Cd^{2+} with receptor by Benesi-Hildebrand plots were found to be $2.874 \times 10^4 \text{ M}^{-1}$ and $6.445 \times 10^4 \text{ M}^{-1}$, respectively. The results indicated the receptor can recognize Ca^{2+} and Cd^{2+} ions from other cations in aqueous solution. Finally, the structure and electronic properties of ligand and its complexes with Ca^{2+} and Cd^{2+} ions were analyzed by DFT and TD-DFT calculations.

Keywords: Azo-azomethine ligand, UV-Vis spectroscopy, Chemosensor, DFT calculations

INTRODUCTION

Calcium is the fifth most abundant element in the human body. This element is responsible for the bone's strength [1]. Calcium ions play a valuable role in cells. They can bind to proteins and activate their catalytic properties [2]. Many biological processes are influenced by calcium. These processes are involved in muscle concentration, exocytosis, neurotransmitter release and steady heartbeat [3,4]. On the other hand, an extra amount of calcium can cause some diseases [5,6]. Therefore, monitoring of calcium concentration is substantial in biological environments. Consequently, the design of selective and sensitive chemosensors for Ca^{2+} has engaged great attention in the past few years [7-10]. Some fluorescence-based receptors such as azacrownethers [11], calix[4]arene [12], polyaminopolycarboxilato [13] and ferrocene derivatives [14,15] have been reported in the literature. However, the

preparation of these sensors is almost difficult. In addition, there are a few sensors that can recognize Ca^{2+} ions and show a high selectivity against most of the other metal ions [16,17].

Cadmium is one of the toxic heavy metals. The high concentration of cadmium metal ions can be harmful to human life and pollute the environment. Cadmium ion can enter organisms, interfere with some metabolic processes and cause some dangerous diseases such as prostate, lung and renal cancers [18-20]. Therefore, the sensitive and selective Cd^{2+} detection has attracted much attention. Some analytical techniques such as atomic absorption spectrometry [21], inductively coupled plasma mass spectrometry (ICP-MS) [22], inductively coupled plasma-atomic emission spectrometry (ICP-AES) [23], electrochemical [24,25] and fluorescent methods [26-29] have been reported for the distinction of cadmium metal ions in past years.

Chemosensors are compounds which can bind selectively to anions, cations and neutral molecules. Among

*Corresponding author. E-mail: shaghghi@azaruniv.ac.ir

chemical receptors, Schiff-base derivatives have been widely considered in past years due to their simple preparation methods. Schiff-bases can be produced by condensation reaction between aldehydes and primary amines. They also interact with a wide range of metal ions. Schiff-bases containing salicyaldimine units and azo groups can be used as effective receptors because they can change the maxima of the absorption band or produce a sensible and significant color change of the solution when bound to cations or anions [30-35].

Considering literature shows that azo-azomethine compounds which are easily prepared can be used as naked-eye sensors for various species including cations, anions and neutral molecules. It means that the investigation of sensor properties of azo-azomethine derivatives does not require sophisticated and expensive analytical instruments. In addition, the nature of substituents and the type of solvent affect different tautomeric forms of these compounds and their selectivity towards different species. Based on what discussed and in continuous to our studies on the sensor properties of azo-azomethine compounds [36-39], we were interested in preparing a new compound of this family and studying its optical properties in the presence of different metal ions. The results showed that the designed ligand can act as a chemosensor for Ca^{2+} and Cd^{2+} ions in a mixture of DMSO/water solution. In addition, density functional theory (DFT) investigations were performed to gain a better understanding of the structure and electronic properties of H_2L and its complexes with Ca^{2+} and Cd^{2+} metal ions. Finally, the electronic spectrum of ligand was analyzed using time-dependent density functional theory (TD-DFT) calculations.

EXPERIMENTAL

Materials and Instruments

4-Bromo-1,2-diaminobenzene, 2-hydroxy benzaldehyde and different metal acetate salts were purchased from Sigma-Aldrich and Merck companies. Solvents with high purity were provided from Merck and used without further purifications. The azophenol precursor (1-(3-formyl-4-hydroxyphenylazobenzene)) was synthesized according to the literature [40]. IR spectra of H_2L and its complexes with Ca^{2+} and Cd^{2+} metal ions recorded using a FT-IR

Spectrometer Bruker Tensor 27 in the region 4000-400 cm^{-1} after mixing the sample with KBr. UV-Vis spectra were recorded with T 60 UV-Vis Spectrometer PG Instruments Ltd. The NMR spectrum of ligand was obtained on Bruker Avance 400 in DMSO with SiMe_4 as the internal standard at room temperature. Elemental analysis was performed on ElementarVario ELIII.

Synthesis of 4-Bromo-1,2-bis[2-hydroxy-5-(phenylazo)benzylideneamino]benzene H_2L

1-(3-Formyl-4-hydroxyphenylazobenzene) (1.77 mmol, 0.400 g) was dissolved in hot ethanol and heated to reflux. Then, a solution of 4-bromo-1,2-diaminobenzene (0.882 mmol, 0.165 g) in ethanol was slowly added to the above solution. After 30 min, the color solution was changed and one orange solid appeared. The reaction continued for 4 h in the reflux condition. Then, the mixture of reaction was filtered, the residue solid washed with ethanol, recrystallized in ethanol-dichloromethane and dried. Yield (0.372 g, 70%). IR (KBr, cm^{-1}) 3421 (-OH), 1610 (-C=N-), 1578, 1525 and 1478 (-N=N- *cis* and *trans*), 1425, 1394, 1282 (CO phenolic), 1191, 1152, 1103, 1048, 999, 964, 895, 860, 837, 805, 764, 710, 689 (C-Br), 643, 605, 499. ^1H NMR (400 MHz, DMSO, d_6): δ 13.41 (s, 2H, OH), 9.17 (d, 2H, ArH, $J = 9.90$ Hz), 8.36 (s, 2H, -HC=N-), 8.01-8.04 (m, 2H, ArH), 7.85 (d, 5H, ArH, $J = 7.99$ Hz), 7.65 (d, 1H, ArH, $J = 8.57$ Hz), 7.53-7.61 (m, 7H, ArH), 7.16 (d of d, 2H, ArH, $J = 2.41$ and 2.37 Hz), Anal. Calc. for $\text{C}_{32}\text{H}_{23}\text{O}_2\text{N}_6\text{Br}\cdot 1.5\text{H}_2\text{O}$: C, 60.95; H, 4.12; N, 13.33. Found: C, 60.98; H, 4.31; N, 13.51, m. p.: 195 °C.

General Methods for the Synthesis of Complexes

H_2L (0.476 mmol, 0.300 g) was dissolved in hot ethanol-dichloromethane mixture and heated to reflux. Then, a solution of $\text{Ca}(\text{CH}_3\text{COO})_2\cdot\text{H}_2\text{O}$ (0.476 mmol, 0.0838 g) or $\text{Cd}(\text{CH}_3\text{COO})_2\cdot 2\text{H}_2\text{O}$ (0.476 mmol, 0.126 g) in ethanol (30 ml) was added to the solution of H_2L during a period of 20 min. Gradually, precipitation was formed after refluxing for about 5 h. Then, the reaction mixture was filtrated. The residue was recrystallized by using ethanol-dichloromethane solvents and dried.

Complex with Ca^{2+} ion (CaL). Orange powder was obtained (0.207 g, Yield: 65%). Decomp: 310 °C, IR (KBr, cm^{-1}) 3063, 1601 (-C=N- imine), 1578, 1520 and 1477

(-N=N- *cis* and *trans*), 1367, 1260 (C-O phenolic), 1190, 1151, 1105, 1020, 900, 864, 834, 807, 766, 687 (C-Br), 602, 503, 436. Elem. Anal. Calc. for C₃₂H₂₁CaO₂N₆Br: C, 61.83; H, 3.38; N, 13.52. Found: C, 61.64; H, 3.27; N, 13.77.

Complex with Cd²⁺ ion (CdL). Orange powder was obtained (0.212 g, Yield: 60%). Decomp: 330 °C, IR (KBr, cm⁻¹) 3061 (OH group), 1607 (-C=N- imine), 1525 and 1480 (-N=N- *cis* and *trans*), 1386, 1262 (C-O phenolic), 1192, 1145, 1104, 1020, 935, 834, 752, 689 (C-Br), 643, 605, 534, 433. Elem. Anal. Calc. for C₃₂H₂₁CdO₂N₆Br: C, 53.84; H, 2.94; N, 11.77. Found: C, 53.60; H, 3.17; N, 11.47.

Theoretical Experiments

DFT calculations were carried out using Gaussian 09 revision D.01 program [41]. Molecular structures were optimized using the B3LYP (Beckes three parameter hybrid functional using the LYP correlation functional) approach in conjunction with the 6-311G basis set for Schiff-base ligand and the LANL2DZ basis set for complexes without any symmetry constrains [42]. To calculate the excited state properties of Schiff base ligand, time-dependent density functional theory (TD-DFT) [43] was employed at the B3LYP/6-311G level using dimethyl sulfoxide as solvent. The excitation energies, oscillator strengths and orbital contribution for the lowest 50 singlet-singlet transitions were calculated on the optimized geometry at ground state.

RESULTS AND DISCUSSIONS

Synthesis and Characterization

The novel azo Schiff base ligand is prepared from the condensation reaction between 4-bromo-1,2-diaminobenzene and 1-(3-formyl-4-hydroxyphenylazobenzene) in ethanol (Scheme 1). The synthesized compound is characterized by FT-IR spectroscopy, ¹H NMR spectroscopy, UV-Vis spectroscopy and elemental analysis. Then, the ability of H₂L for the detection of some transition and main metal ions is investigated by UV-Vis spectroscopy. As will be discussed, H₂L can highly recognize Ca²⁺ and Cd²⁺ metal ions in aqueous solution. Finally, to study the binding sites of ligand, calcium and cadmium complexes with H₂L are synthesized and

investigated by some common techniques.

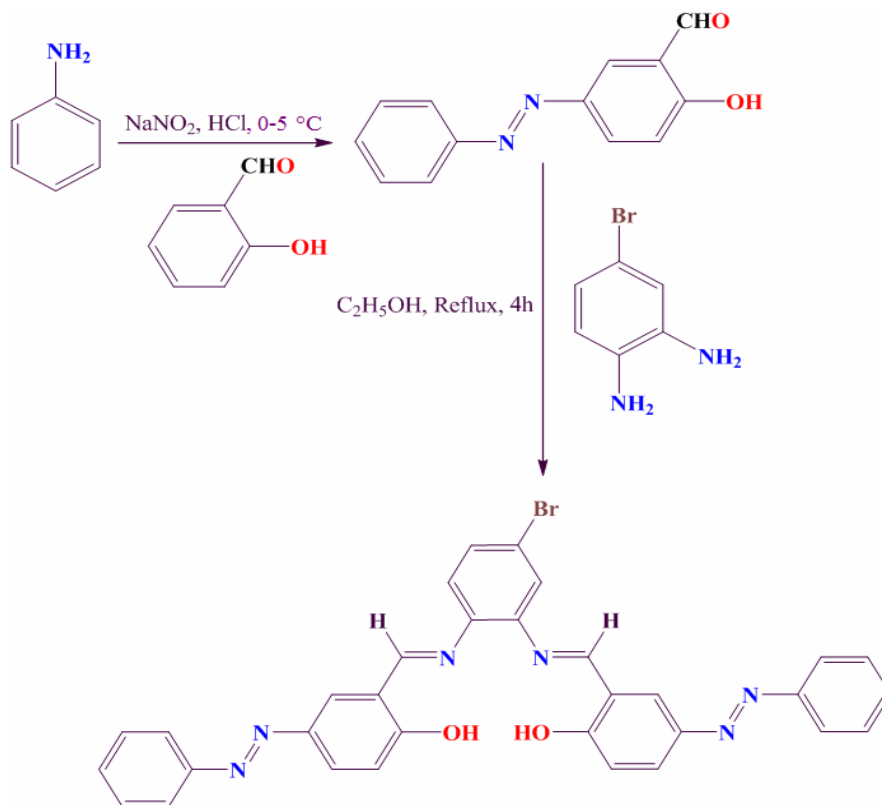
FT-IR spectra. The appearance of a strong and sharp absorbance peak in 1610 cm⁻¹ for imine stretching vibration in the IR spectrum of H₂L indicates the formation of azo Schiff-base ligand. Moreover, the vibration of *cis* and *trans* azo groups appears at 1525 cm⁻¹ and 1478 cm⁻¹, respectively. Also, the stretching vibration of the C-Br bond is observed as sharp and medium absorption peak at 689 cm⁻¹ [44,45]. After complexation with calcium and cadmium metal ions, the absorbance of imine vibrations shifts to shorter wavenumbers about 3-9 cm⁻¹ and decreases in intensity. This suggests the coordination of electron pair of nitrogen atoms of imine groups to the metal ion center. Also, disappearing of -OH stretching vibration in the IR spectra of the complexes reveals that hydroxyl groups are deprotonated when bound to calcium or cadmium metal ions (see Fig. 1).

¹H NMR spectra. In the ¹H NMR spectrum of ligand, the imine and phenolic -OH protons appear at δ = 8.36 and δ = 13.42 ppm as singlet resonances, respectively. In addition, aromatic protons are observed in the 7.15-9.19 ppm region (see Fig. 2).

Molar conductivity. The molar conductivity values of H₂L and its complexes with calcium and cadmium metal ions show that both complexes are non-electrolyte (Table 1). It means that H₂L acts as one dianionic tetradentate ligand with a N₂O₂ core when bound to the metal ion center. These results reveal a good agreement with FT-IR and elemental analysis data.

UV-Vis Experiments

UV-Vis spectrum of ligand. UV-Vis spectra of H₂L in DMSO and DMSO/water (9:1) solvents are shown in Fig. 3. The azo-azomethine ligand shows π→π* transition of aromatic rings, π→π* and n→π* transitions of imine groups and π→π* and n→π* transitions of azo units in DMSO. H₂L reveals one sharp absorption band at λ = 266 nm, assigned to the π→π* transition of aromatic rings, one absorption shoulder at λ = 322 nm corresponding to the π→π* transition of imine groups, one broad absorption band at λ = 347 nm attributable to the n→π* transition of imine groups and π→π* transition of azo units and finally one broad absorption band at λ = 447 nm corresponding to the n→π* transition of azo groups [43,44] (the width of



Scheme 1. The Synthesis route and structure of H₂L

absorption band at 347 nm indicates $\pi \rightarrow \pi^*$ or $n \rightarrow \pi^*$ transitions of imine groups probably overlaps with $\pi \rightarrow \pi^*$ transition of azo units). The UV-Vis spectrum of H₂L in DMSO/water (9:1) shows main band at around 351 nm which can be related to the $\pi \rightarrow \pi^*$ transition of azo groups. According to our studies, the solvatochromism exhibited by azo ligands may be due to the effect of proton transfer or dipole moment changes in various solvents. In DMSO, an additional maximum absorption observed at 447 nm is attributed to the existence of the tautomeric form [39,45,46].

UV-Vis spectra for cation sensing. The ability of H₂L for recognition of Ca²⁺, Cd²⁺, Cu²⁺, Hg²⁺, Ag⁺, Pb²⁺, Zn²⁺, Na⁺ and DMSO:H₂O (9:1) as acetate salts is investigated. As shown in Fig. 4, upon incremental addition of Ca²⁺ and Cd²⁺ metal ions to H₂L solution, the absorption band at 351 nm strongly decreases in intensity (about for Ca²⁺ ion, approximately disappears) and one new broad absorption

band appears for each metal ions in 430-450 nm region. Whereas, other metal ions cause no sensible change in the absorption spectra. It is well known that azophenol groups in different compounds may exist in azophenol and quinone-hydrazone tautomeric forms. There are many factors affecting equilibrium tautomeric forms such as structure, temperature, solvent and complexation with metal ions [50-53]. In this case, it seems that complexation of Ca²⁺ and Cd²⁺ with H₂L affects keto-enol equilibrium. The increase in absorption intensity around 450 nm after adding Ca²⁺ and Cd²⁺ to the ligand solution could be related to the metal complexation-induced release of protons of azophenol units to the quinone-hydrazone tautomer [51-53], although it is unknown that why among the tested metal ions, Ca²⁺ and Cd²⁺ have the highest effect on keto-enol equilibrium.

Upon progressive addition of Ca²⁺ ions to ligand solution, the peak at 351 nm gradually decreases in intensity and one new absorption band appears at 450 nm. The new

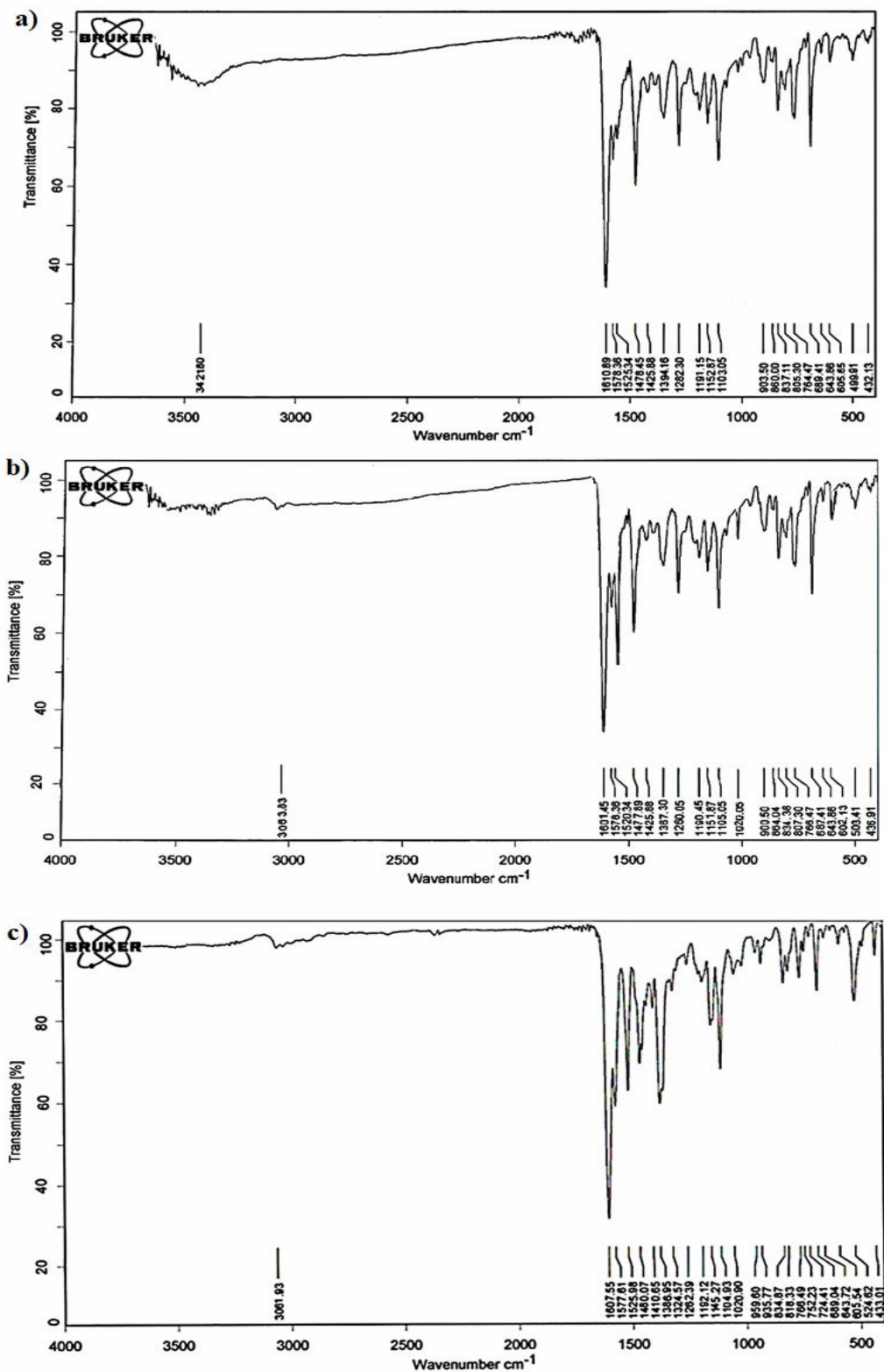


Fig. 1. FT-IR spectra of H₂L (a), CaL (b) and CdL (c).

Table 1. Molar Conductivity Values for Ligand and Complexes (10^{-3} M in DMSO)

Compound	Molar conductivity ($\text{cm}^2 \Omega^{-1} \text{mol}^{-1}$)
DMSO	1.475
H ₂ L	1.625
CaL	1.661
CdL	1.764

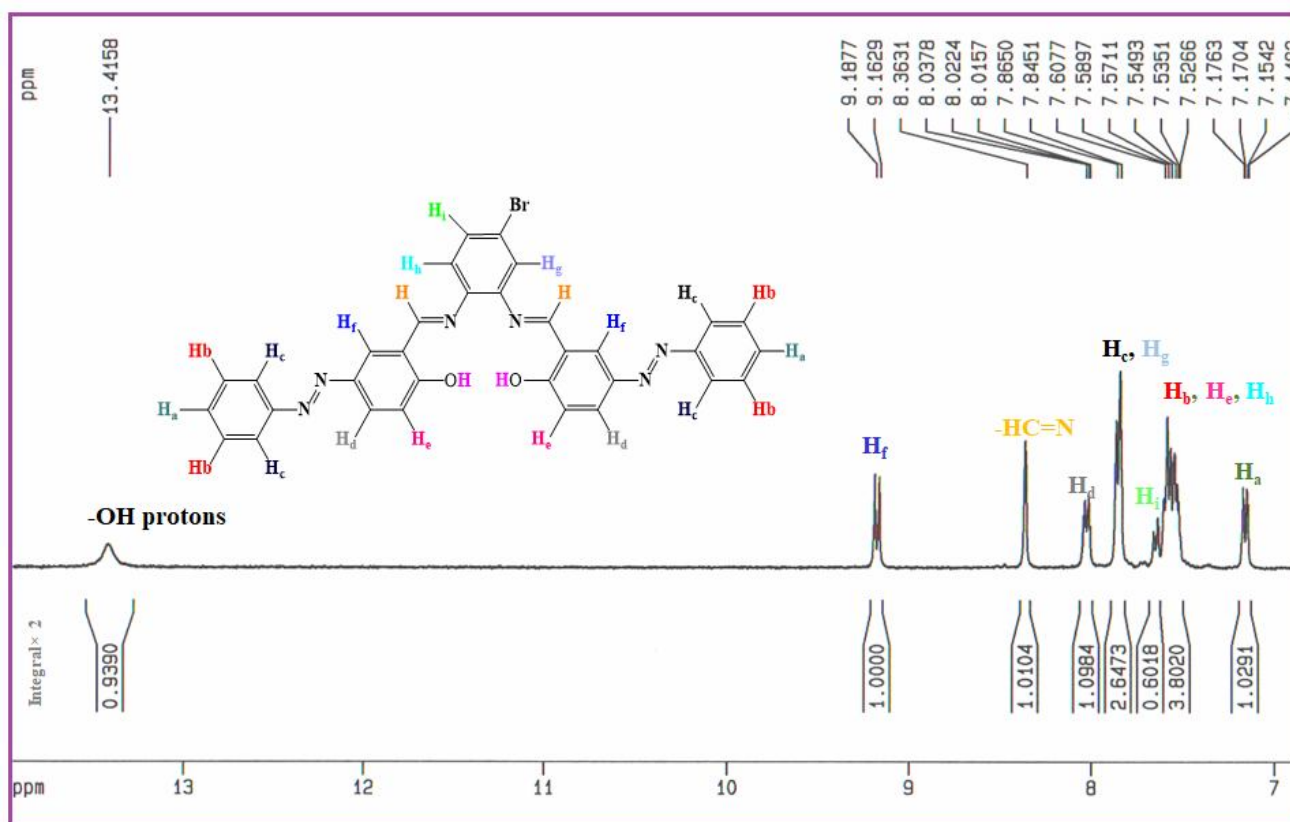


Fig. 2. ^1H NMR spectrum of H₂L.

band gradually rises in intensity with the incremental addition of Ca^{2+} (Fig. 5). Also, upon continuous addition of Cd^{2+} ions to H₂L, a new absorption band is produced at 441 nm with a hypsochromic shift and the peak at 351 nm

progressively shrinks in intensity (Fig. 6). The appearance of an Isobestic point at 369 nm for Ca^{2+} and at 379 nm for Cd^{2+} indicates the formation of only one active complex with the receptor. In the next step, the 1:1 binding-

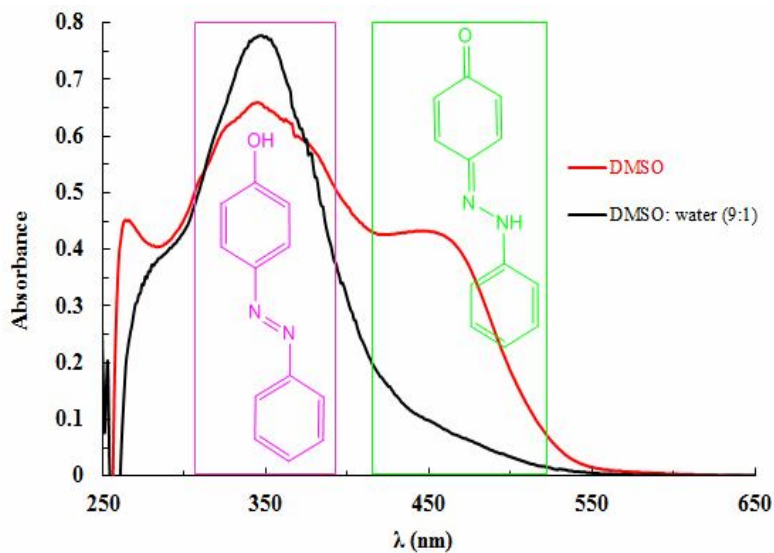


Fig. 3. UV-Vis spectra of H_2L in DMSO and DMSO:H $_2$ O (9:1) solvents (2×10^{-5} M).

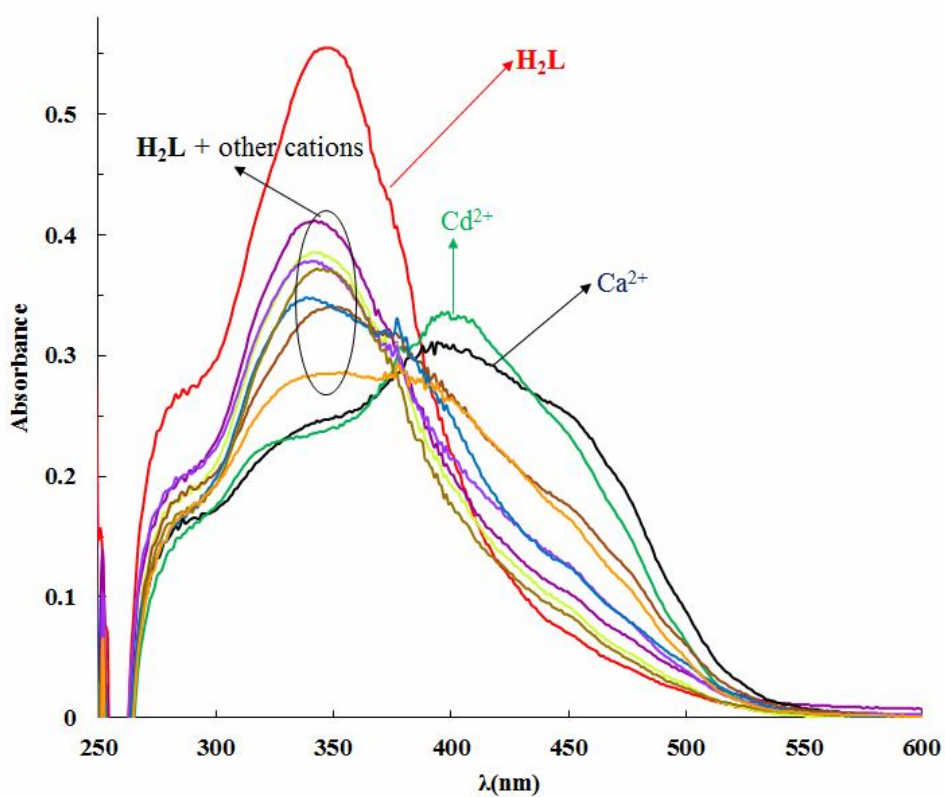
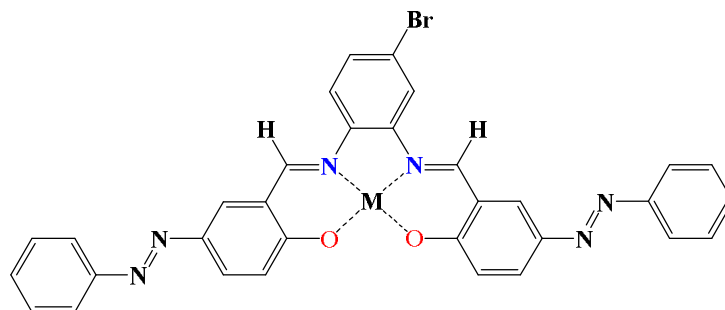


Fig. 4. UV-Vis spectra of H_2L (2×10^{-5} M) in the presence of different metal ions (Ca^{2+} , Cd^{2+} , Cu^{2+} , Ni^{2+} , Zn^{2+} , Hg^{2+} , Pb^{2+} , Ag^+ and Na^+) as their acetate salts (2×10^{-5} M) in DMSO/water (9:1).



Scheme 2. The proposed structure for H₂L with Ca²⁺ and Cd²⁺ metal ions

Table 2. The UV-Vis Spectra Data for Titration of H₂L with Ca²⁺ and Cd²⁺ Metal Ions in DMSO:H₂O (9:1)

H ₂ L + cation	Ligand, λ _{max} (nm)	Complex, λ _{max} (nm)	Bathochromic shift, Δλ _{max} (nm)	K _a (M ⁻¹)
H ₂ L-Ca ²⁺	347	450	103	2.874 × 10 ⁴
H ₂ L-Cd ²⁺	347	441	94	6.445 × 10 ⁴

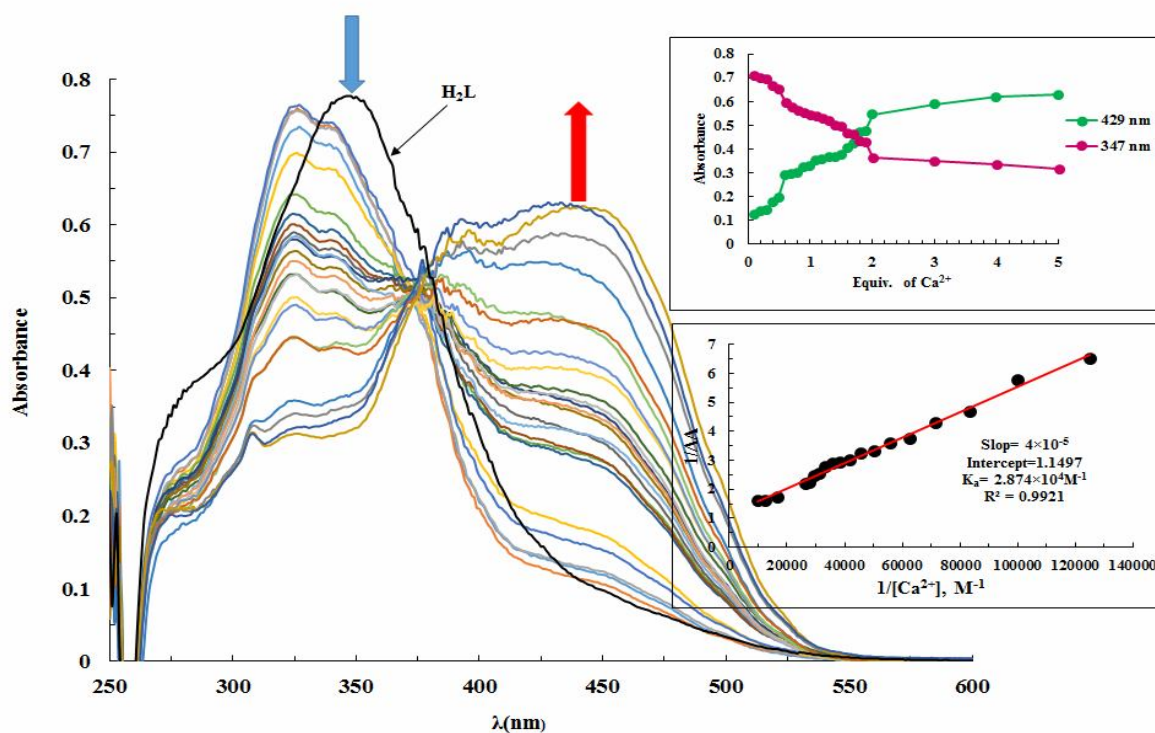


Fig. 5. Absorption spectra changes of H₂L (2×10^{-5} M) after addition of 0.1-5 eq of Ca²⁺ metal ion in DMSO:H₂O (9:1). Insets: above; Absorption at selected wavelengths *versus* different equivalent of Ca²⁺, down: Benesi-Hildebrand plot for H₂L with Ca²⁺ ion.

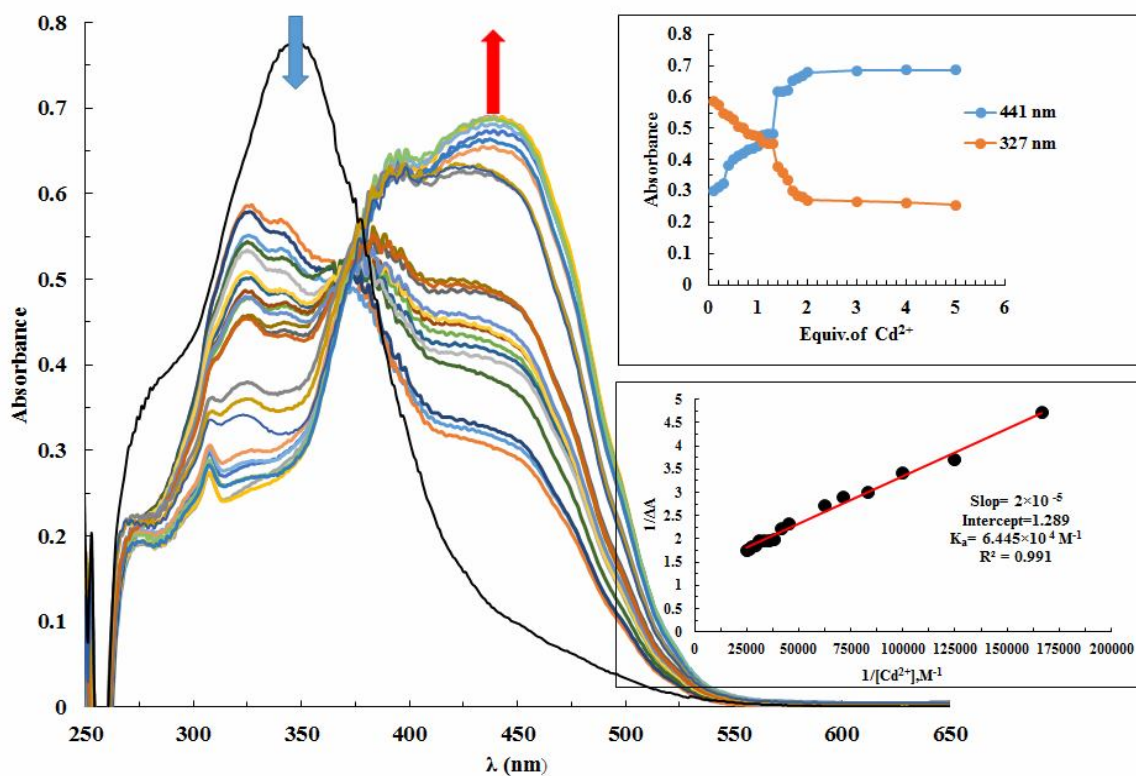


Fig. 6. Absorption spectra changes of H_2L (2×10^{-5} M) after addition of 0-5 eq of Cd^{2+} metal ion in DMSO:H $_2$ O (9:1). Insets: above; Absorption at selected wavelengths *versus* different equivalent of Cd^{2+} , down: Benesi-Hildebrand plot for H_2L with Cd^{2+} ion.

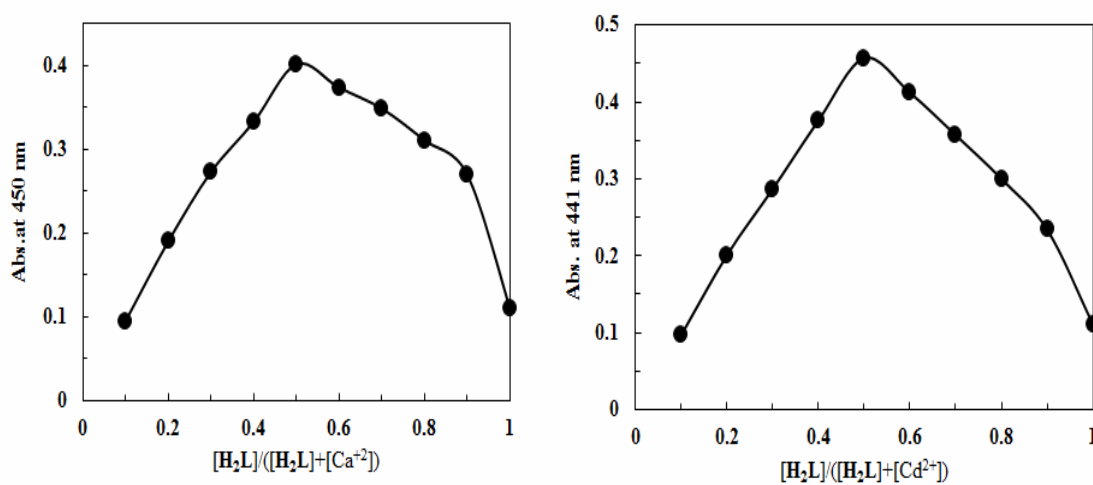


Fig. 7. The Job plots for the complexes of H_2L with Ca^{2+} and Cd^{2+} ions.

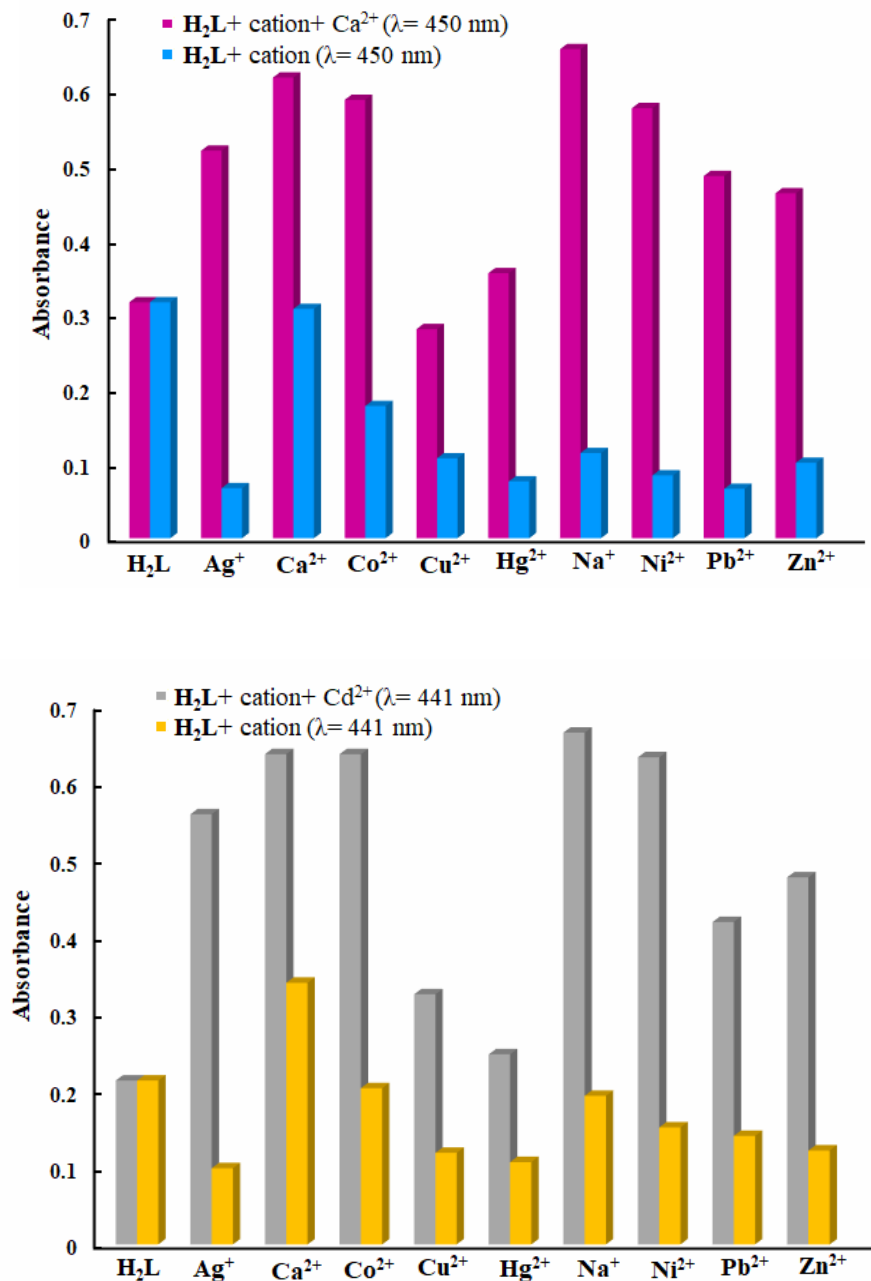


Fig. 8. Effect of competitive cations on the interaction between H₂L and Ca²⁺ or Cd²⁺ ions.

stoichiometry for H₂L with Ca²⁺ and Cd²⁺ ions is obtained by using the Job method (Fig. 7). Consequently, H₂L acts as one tetradentate ligand with O and N donor atoms when bound to the Ca²⁺ or Cd²⁺ metal ions (Scheme 2). Moreover, 1:1 association constants of H₂L with Ca²⁺ and

Ca²⁺ are calculated using the Benesi-Hildebrand method [54]. The results of titration of the receptor with Ca²⁺ and Cd²⁺ metal ions are given in Table 2.

Competition experiments. The selectivity of H₂L is investigated for the detection of Ca²⁺ and Cd²⁺ ions in the

Table 3. Effect of Interfering Different Ions on the Intraction between H₂L and Ca²⁺ ([Cation]/[Ca²⁺] = 10)

Cation	A ^a	A ₀ ^b	A/A ₀	RSD (%) ^c
Cd ²⁺	0.617	0.307	2.01	1.370
Co ²⁺	0.587	0.177	3.32	1.382
Cu ²⁺	0.28	0.107	2.62	1.630
Hg ²⁺	0.355	0.076	4.60	0.715
Pb ²⁺	0.485	0.066	7.35	0.521
Zn ²⁺	0.462	0.101	4.57	0.765
Ni ²⁺	0.576	0.084	6.85	1.497
Ag ⁺	0.519	0.067	7.74	0.776
Na ⁺	0.655	0.114	5.74	0.554

^aAbsorbance of [H₂L] + [cation] + [Ca²⁺] at 450 nm. ^bAbsorbance of [H₂L] + [cation] at 450 nm and ^cRSD% for average of three measurements.

Table 4. Effect of Interfering Different Ions on the Intraction between H₂L and Cd²⁺ ([Cation]/[Cd²⁺] = 10)

Cation	A ^a	A ₀ ^b	A/A ₀	RSD (%) ^c
Ca ²⁺	0.637	0.340	1.87	0.748
Co ²⁺	0.635	0.201	3.16	0.799
Cu ²⁺	0.325	0.119	2.73	1.926
Hg ²⁺	0.247	0.107	2.31	1.952
Pb ²⁺	0.419	0.141	2.97	1.076
Zn ²⁺	0.477	0.122	3.91	0.856
Ni ²⁺	0.633	0.152	4.16	0.801
Ag ⁺	0.559	0.099	5.64	1.567
Na ⁺	0.665	0.193	3.39	0.746

^aAbsorbance of [H₂L] + [cation] + [Cd²⁺] at 441 nm. ^bAbsorbance of [H₂L] + [cation] at 441 nm and ^cRSD% for average of three measurements.

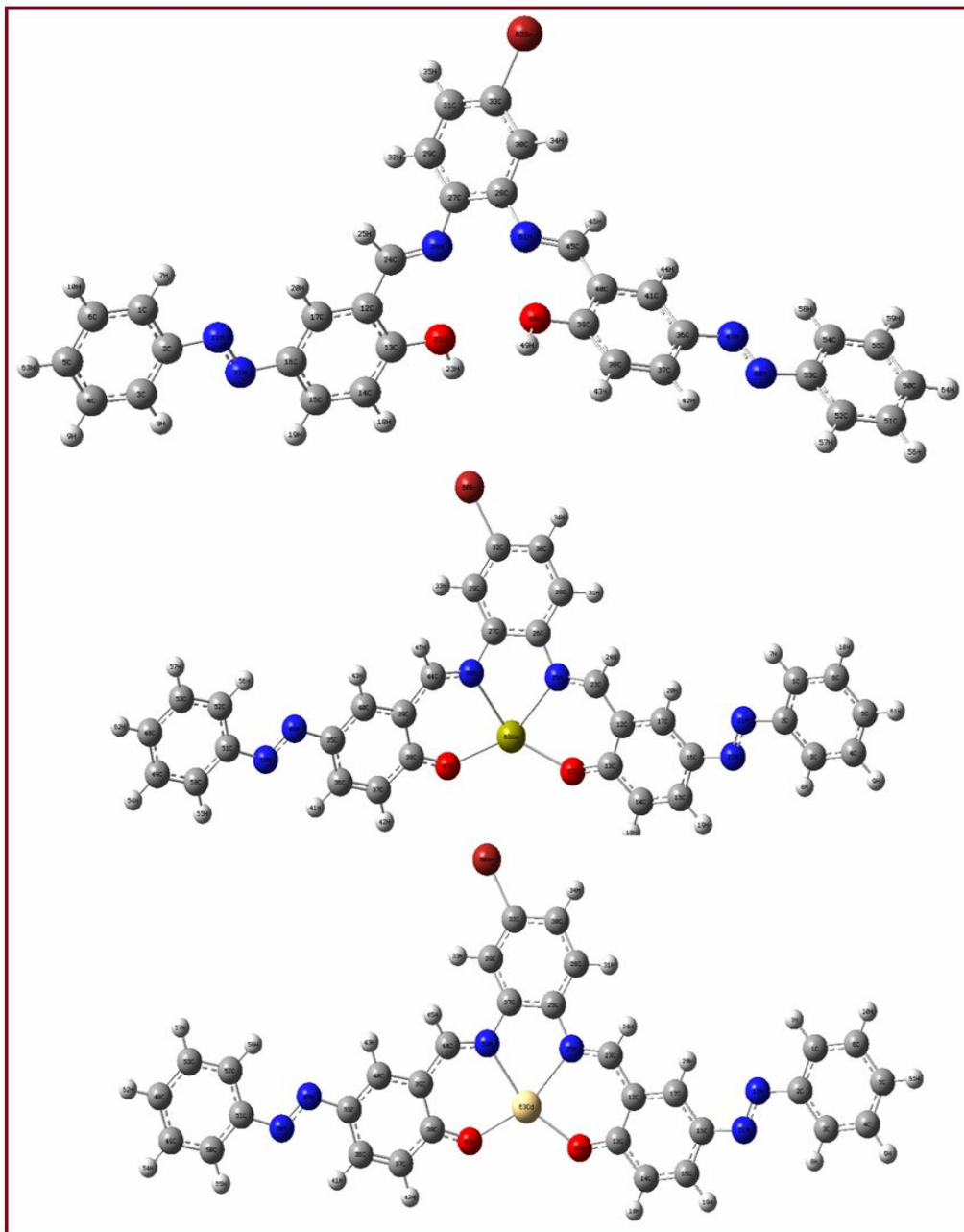


Fig. 9. Optimized geometry of H₂L and its complexes with Ca²⁺ and Cd²⁺ metal ions.

presence of Co²⁺, Cu²⁺, Hg²⁺, Pb²⁺, Zn²⁺, Ni²⁺, Ag⁺ and Na⁺ metal ions. H₂L (2×10^{-5} M) reacts with Ca²⁺ (2×10^{-5} M) or Cd²⁺ (2×10^{-5} M) in the presence of excess competing metal ions (2×10^{-4} M) in DMSO:H₂O (9:1). The results

are summarized in Fig. 8 and Tables 3 and 4. As indicated, almost other metal ions produce no perturbation for the detection of Ca²⁺ or Cd²⁺ ions in the aqueous solution. Consequently, Azo Schiff base H₂L has a high ability for

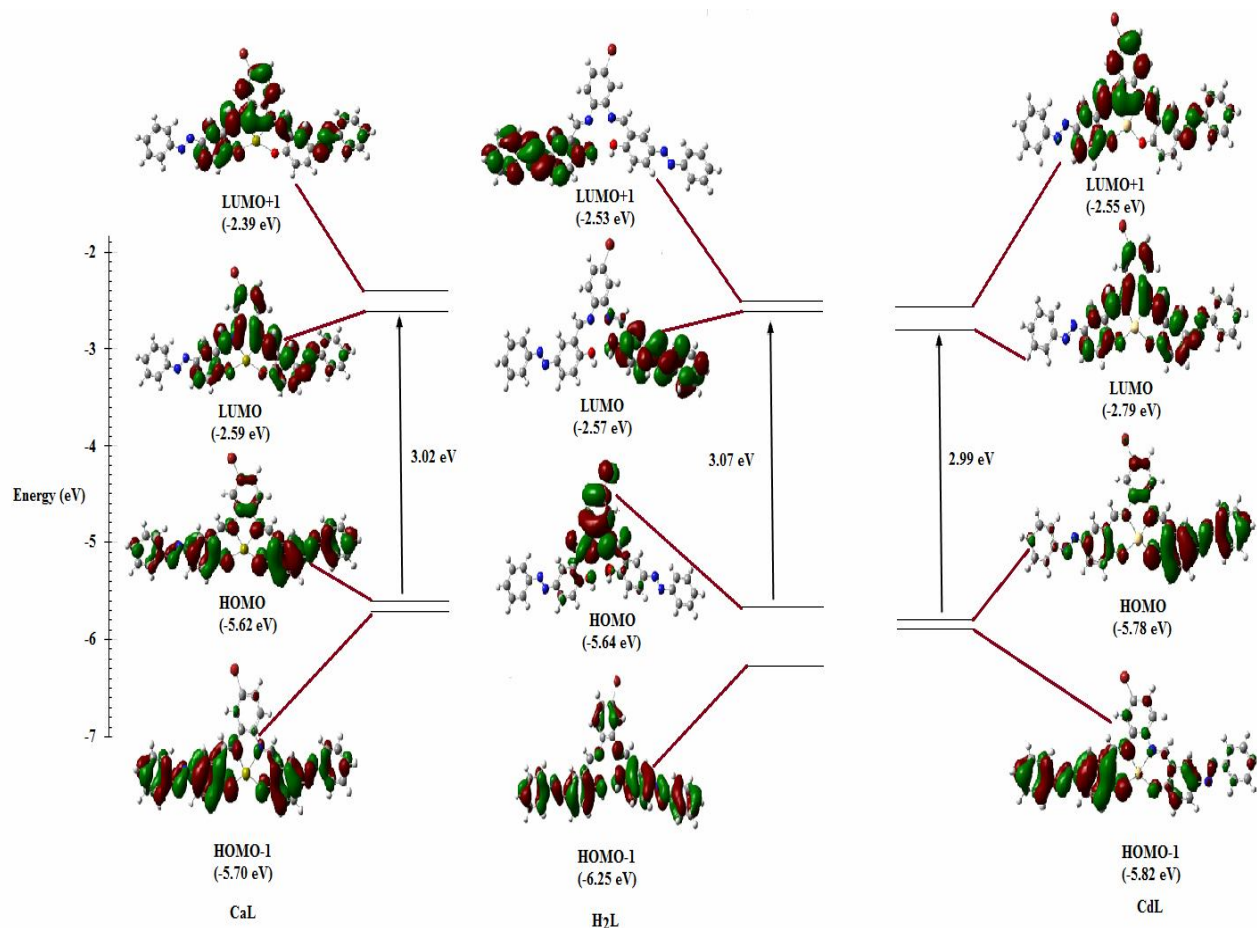


Fig. 10. Molecular orbital diagrams of H₂L and its complexes with Ca²⁺ and Cd²⁺ metal ions by DFT method.

the recognition of Ca²⁺ and Cd²⁺ metal ions in aqueous solutions.

Theoretical Studies

In this section, the structure and electronic properties of ligand and its complexes with calcium and cadmium metal ions are studied by DFT calculations [55]. The fully optimized molecular structure of the compounds is shown in Fig. 9. Also, molecular orbital diagrams of them is given in Fig. 10. Analysis of the frontier molecular orbitals of ligand and its complexes with Ca²⁺ and Cd²⁺ metal ions indicates that the band gap energies are 3.07, 3.02 and 2.99 eV, respectively.

UV-Vis spectrum of ligand by TD-DFT calculations.

To predict the electronic spectrum of H₂L, TD-DFT

calculations are performed on the ground state of its optimized structure [55]. Some electronic transitions for ligand are given in Table 5. The important electronic transitions of H₂L, obtained from TD-DFT calculations, are: fifth excited state at 406 nm with oscillator strength of 0.4135, corresponding to electron excitation from HOMO to LUMO+2 (78%), sixth excited state at 371 nm with oscillator strength of 1.1206 related to electron excitation from HOMO-2 to LOMO+1 (29%), HOMO-1 to LOMO (22%) and HOMO-1 to LOMO+1 (38%), twenty-second excited state at 308 nm with oscillator strength of 0.1448 due to electron excitation from HOMO-9 to LUMO (13%), HOMO-6 to LUMO (46%) and HOMO-1 to LUMO+3 (11.5%), and forty-second excited state at 259 nm with oscillator of strength 0.2573, corresponding to electron

Table 5. Some UV-Vis Data Calculated at the TD-DFT Level for H₂L in DMSO

Excited state	λ_{\max} (nm) (Experimental)	λ_{\max} (nm) (Calculated)	E (eV)	Oscillator strength (f)	Major contributions
5	447	406	3.0515	0.4135	HOMO→LUMO (13%) HOMO→LUMO+2 (78%)
6	347	371	3.3430	1.1206	HOMO-2→LUMO+1 (29%) HOMO-1→LUMO (22%) HOMO-1→LUMO+1 (38%)
7		369	3.3642	0.4793	HOMO-2→LUMO (33%) HOMO-1→LUMO (47%)
8		364	3.4067	0.1728	HOMO-2→LUMO (56%) HOMO-1→LUMO (27%)
14		332	3.7380	0.1358	HOMO-5→LUMO+1 (11%) HOMO-2→LUMO+2(16.5%) HOMO-1→LUMO+2 (50%)
22	322	308	4.0289	0.1448	HOMO-9→LUMO (13%) HOMO-6→LUMO (46%) HOMO-1→LUMO+3 (11.5%)
24		292	4.2504	0.1581	HOMO-6→LUMO (21%) HOMO-2→LUMO+3 (10%) HOMO-1→LUMO+3 (60%)
30		279	4.4505	0.1197	HOMO-6→LUMO+2 (30%) HOMO-5→LUMO+3 (27.5%)
36		269	4.6061	0.1507	HOMO-6→LUMO+2 (36%) HOMO-5→LUMO+3 (29%) HOMO→LUMO+4 (12%)
42	266	259	4.7927	0.2573	HOMO-12→LUMO (6.5%) HOMO-9→LUMO+2 (66%)

excitation from HOMO-9 to LUMO+2 (66%) and HOMO-12 to LUMO (6.5%). The fifth excitation state can be attributed to the absorption band at 447 nm in the

experimental spectrum of H₂L. In this manner, sixth, twenty-second and forty-second excitation states can be related to the absorption bands at 347 nm, 322 nm and

266 nm in the experimental spectrum, respectively.

CONCLUSIONS

One new azo-azomethine chemosensor for the detection of Ca^{2+} and Cd^{2+} metal ions was synthesized from the condensation reaction between 4-bromo-1,2-diaminobenzene and 1-(3-formyl-4-hydroxyphenylazobenzene) in ethanol. The prepared compound was characterized by standard and common techniques. The named metal ions produced sensible changes in the UV-Vis spectrum of ligand. The results of the competition experiments indicated that the chemosensor could selectively recognize Ca^{2+} and Cd^{2+} metal ions in aqueous solution. Finally, the structure and electronic properties of ligand and its complexes were studied using DFT investigations. Analysis of the electronic spectrum of the ligand, using TD-DFT calculations, revealed a good agreement between the theoretical and experimental data.

ACKNOWLEDGMENTS

The authors are grateful to Azarbaijan Shahid Madani University for financial support of this project.

REFERENCES

- [1] H. Sigel, A. Sigel, *Metal Ions in Biological Systems*. vol. 17: Calcium and its Role in Biology. Dekker M. New York, 1984.
- [2] M.E. Shills, *Modern Nutrition in Health and Disease*. 10th ed. Philadelphia: Lippincott, Williams and Wilkins, 2006.
- [3] G.A. Augustine, *Curr. Opin. Neurobiol.* 11 (2001) 320.
- [4] M.A. Fowler, G.L. Smith, *Appl. Physiol.* 107 (2009) 1981.
- [5] P. Munro, *Clin J. Am. Soc. Nephrol.* 5 (2010) S23.
- [6] D. Papandreou, P. Malindretos, Z. Karabouta, I. Rouso, *Int. J. Endocrinol.* 2010 (2009) 1.
- [7] R. Sahli, N. Raouafi, E. Maisonhaute, K. Boujlela, B. Schöllhorn, *Electrochim. Acta* 63 (2012) 228.
- [8] J. An, Z. Yang, M. Yan, T. Li, *J. Lumin.* 139 (2013) 79.
- [9] S.R. Ankireddy, J. Kim, *Sens. Actuators, B* 225 (2018) 3425.
- [10] E. Johna, C. Chengb, A. Bornschlegel, O. Brüggemann, T. Posnicek, M. Brandl, *Sens. Actuators, B* 209 (2015) 1023.
- [11] R. Velu, V.T. Ramakrishnan, P. Ramamurthy, *Tetrahedron Lett.* 51 (2010) 4331.
- [12] K.C. Chang, I.H. Su, G.H. Lee, W.S. Chung, *Tetrahedron Lett.* 48 (2007) 7274.
- [13] U. Norizaki, T. Kazuyuki, O. Akira, O. Taka-aki, Y. Hitoshi, *Macromol. Symp.* 186 (2002) 129.
- [14] B. Delavaux-Nicot, J. Maynadie', D. Lavabre, S. Fery-Forgues, *J. Organomet. Chem.* 692 (2007) 874.
- [15] B. Delavaux-Nicot, J. Maynadie, D. Lavabre, S. Fery-Forgues, *J. Organomet. Chem.* 692 (2007) 3351.
- [16] E. Arunkumar, P. Chithra, A. Ajayaghosh, *J. Am. Chem. Soc.* 126 (2004) 6590.
- [17] E. Arunkumar, A. Ajayaghosh, J. Daub, *J. Am. Chem. Soc.* 127 (2005) 3156.
- [18] G. Jiang, L. Xu, S. Song, C. Zhu, Q. Wu, L. Zhang, L. Wu, *Toxicology* 244 (2008) 49.
- [19] R. Goyer, J. Liu, M. Waalkes, *Biometals.* 17 (2004) 555.
- [20] J. Godt, F. Scheidig, C. Grosse-Siestrup, V. Esche, P. Brandenburg, A. Reich, D.A. Groneberg, *J. Occup. Med. Toxicol.* 1 (2006) 1.
- [21] H. Parham, N. Pourreza, N. Rahbar, *J. Hazard. Mater.* 163 (2009) 588.
- [22] S. D'Ilio, F. Petrucci, M. D'Amato, M. Di Gregorio, O. Senofonte, N. Violante, *Anal. Chim. Acta* 624 (2008) 59.
- [23] M. Zougagh, A.G. Torres, J.M.C. Pavon, *Talanta.* 56 (2002) 753.
- [24] O. Krystofova, L. Trnkova, V. Adam, J. Zehnalek, J. Hubalek, P. Babula, R. Kizek, *Sensors* 10 (2010) 5308.
- [25] T. Priya, N. Dhanalakshmi, S. Thennarasu, N. Thinakaran, *Carbohydr. Polym.* 182 (2018) 199.
- [26] X. Liu, N. Li, M.M. Xu, C. Jiang, J. Wang, G. Song, Y. Wang, *Spectrochim. Acta, Part A* 208 (2019) 236.
- [27] P. Wang, D. Zhou, B. Chen, *Spectrochim. Acta, Part A* 207 (2019) 276.
- [28] Z.N. Lu, L. Wang, X. Zhang, Z.J. Zhu, *Spectrochim. Acta, Part A* 213 (2019) 57.

- [29] Y. Liu, Q. Qiao, M. Zhao, W. Yin, L. Miao, L. Wang, Z. Xu, *Dyes Pigm.* 133 (2016) 339.
- [30] Z. Li, S. Wang, L. Xiao, X. Li, X. Jing, X. Peng, L. Ren, *Inorg. Chim. Acta* 479 (2018) 148.
- [31] R. Arabahmad, *Talanta* 194 (2019) 119.
- [32] S. Gholizadeh Dogaheh, H. Khanmohammadi *Spectrochim. Acta, Part A* 179 (2017) 32.
- [33] G. Kurtoglu, B. Avar, H. Zengin, M. Kose, K. Sayin, M. Kurtoglu, *J. Mol. Liq.* 200 (2014) 105.
- [34] A.K. Manna, J. Mondal, R. Chandra, K. Rout, G.K. Patra, *Anal. Methods* 10 (2018) 2317.
- [35] S. Banerjee, S.P. Brandão, A. Saha, *RSC Adv.* 6 (2016) 101924.
- [36] B. Shaabani, Z. Shaghghi, A.A. Khandar, *Spectrochim. Acta, Part A* 98 (2012) 81.
- [37] Z. Shaghghi, *Spectrochim. Acta, Part A* 131 (2014) 67.
- [38] Z. Shaghghi, R. Rezanezhad, *Chemistry Select.* 3 (2018) 5534.
- [39] Z. Shaghghi, G. Dehghan, *Acta. Chim. Slov.* 65 (2018) 670.
- [40] A.A. Khandar, Z. Rezvani, *Polyhedron* 18 (1999) 129.
- [41] M.J. Frisch, *et al.*, *Gaussian 09*, Revision D.01, Gaussian Inc, Wallingford CT, 2004.
- [42] C. Lee, W. Yang, R.G. Parr, *Phys. Rev. B* 17 (1988) 785.
- [43] E. Gross, W. Kohn, *Adv. Quant. Chem.* 21 (1990) 255.
- [44] A.N. Kursunlu, E. Guler, F. Sevgi, B. Ozkalp, *J. Mol. Struct.* 1048 (2013) 476.
- [45] M.S. More, S.B. Pawal, S.R. Lolage, S.S. Chavan, *J. Mol. Struct.* 1128 (2017) 419.
- [46] H. Galen, G. Hennrich, J.D. Mendoza, P. Prados, *Eur. J. Org. Chem.* (2010) 1249.
- [47] R. Arab Ahmadi, S. Amani, *Molecules* 17 (2012) 6434.
- [48] H. Khanmohammadi, M. Pass, K. Rezaeian, G. Talei, *J. Mol. Struct.* 1072 (2014) 232.
- [49] H. Khanmohammadi, A. Abdollahi, *Dyes Pigm.* 94 (2012) 163.
- [50] K.T. Smith, S.C. Young, G.W. DeBlasio, C.S. Hamann, *J. Chem. Educ.* 93 (2016) 790.
- [51] T.H. Kim, S.H. Kim, L.V. Tan, Y.G. Seo, S.Y. Park, H. Kim, J.S. Kim, *Talanta* 71 (2007) 1294.
- [52] Y. Dong, T.H. Kim, H.J. Kim, M.H. Lee, S.Y. Lee, R.K. Mahajan, H. Kim, J.S. Kim, *J. Electroanal. Chem.* 628 (2009) 119.
- [53] T.H. Kim, S.H. Kim, L.Y. Tan, Y. Dong, H. Kim, J.S. Kim, *Talanta* 74 (2008) 1654.
- [54] T.L. Kao, C.C. Wang, Y.T. Pan, Y.J. Shiao, J.Y. Yen, C.M. Shu, G.H. Lee, S.M. Peng, W.S. Chung, *J. Org. Chem.* 70 (2005) 2912.
- [55] S.G. Niyaky, M. Montazerzohori, A. Masoudiasl, J.M. White, *J. Mol. Struct.* 1131 (2017) 201.